DEVELOPMENT OF NANOCATALYSTS FOR THE SYNTHESIS OF BIOFUELS FROM BIOMASS DERIVED SYNGAS

Final Report

KLK769

N12-05

National Institute for Advanced Transportation Technology

University of Idaho

Guanqun Luo, Pavel Bakharev, Armando McDonald,

David McIlroy

June 2012

DISCLAIMER

The contents of this report reflect the views of the authors, who are responsible for the facts and the accuracy of the information presented herein. This document is disseminated under the sponsorship of the Department of Transportation, University Transportation Centers Program, in the interest of information exchange. The U.S. Government assumes no liability for the contents or use thereof.

1. Report No.	2. Government Accession No.	3. Recipient's Catalog No.
4. Title and Subtitle Development of Nanocatalysts for the Synthesis of Biofuels from Biomass Derived Syngas		5. Report Date June 2012
		6. Performing Organization Code Budget KLK769
7. Author(s) McDonald, Dr. Armando; Guanqun, Luo; McIlroy, Dr. David; Bakharev, Pavel		8. Performing Organization Report No. N12-05
9. Performing Organization Name and Address National Institute for Advanced Transportation Technology University of Idaho PO Box 440901; 115 Engineering Physics Building Moscow, ID 83844-0901		10. Work Unit No. (TRAIS) 11. Contract or Grant No. DTRT07-G-0056
12. Sponsoring Agency Name and Address US Department of Transportation Research and Special Programs Administration 400 7th Street SW Washington, DC 20509-0001		13. Type of Report and Period Covered Final Report: August 2011 – June 2012 14. Sponsoring Agency Code USDOT/RSPA/DIR-1
15. Supplementary Notes:		

16. Abstract

The potential silica nanospring (NS) supported cobalt catalyst (Co/SiO_2-NS) for Fischer-Tropsch synthesis (FTS) was investigated, and the results were compared with those of a conventional silica gel supported cobalt catalyst (Co/SiO_2-gel). Co/SiO_2-gel and Co/SiO_2-NS catalysts were prepared using the incipient wetness impregnation method and a thermal assisted reduction process, respectively, and characterized by scanning electron microscopy/ energy dispersive spectroscopy (SEM/EDS), transmission electron microscopy (TEM), N_2 physisorption, X-ray powder diffraction (XRD), and H_2-temperature programed reduction (H_2-TPR). The catalysts were evaluated for their conversion of syngas to products in a quartz fix-bed micro-reactor (230 °C, atm pressure). The FTS products were trapped and characterized by GC-MS to determine conversion efficiency. The products (alkanes) for both catalysts ranged from C1 to C21 and would be a suitable substrate for diesel. The results show that the NS approach for a FTS catalyst support shows promise for generating fuels from syngas. Future work will focus on optimizing Co/SiO_2-NS catalyst for improved conversion efficiencies.

17. Key Words	18. Distribution Statement
Biofuels (or biomass fuels); Gasification; Catalysis	Unrestricted; Document is available to the public through the National Technical Information Service; Springfield, VT.

19. Security Classif. (of this report)	20. Security Classif. (of this page)	21. No. of Pages	22. Price
Unclassified	Unclassified	21	…

Form DOT F 1700.7 (8-72) Reproduction of completed page authorized

TABLE OF CONTENTS

FIGURES

TABLES

EXECUTIVE SUMMARY

Converting under-utilized biomass from forestry and agricultural sectors to biofuels would benefit the nation's energy security by displacing imported petroleum. More than three million tons/y of biomass is available in the Pacific Northwest (PNW) alone (Skog et al. 2008). This level of biomass could theoretically produce five million barrels/y of biofuels. Production of high yields of syngas and upgrading into "drop-in" fuels still requires research, particularly regarding feedstocks and catalyst development. Upgrading biomass-derived syngas to biofuels opens opportunities for near-term commercial development and use in petroleum refineries.

We tested the hypothesis that Fischer-Tropsch (FT) type catalytic surfaces can be grown on nanospring (NS) -supported structures, which results in high accessibility of the syngas for enhanced conversion into biofuels. This proof of principle study has proven that NS-catalyst can produce "drop-in" biofuels. We also were successful in developing a micro-reactor system for catalyst and product evaluation for future studies.

Other outcomes of this project were (i) to support and train two graduate students in the art of catalyst development, biofuels synthesis, and characterization, (ii) to submit an invention disclosure (provisional patent) on the nanocatalyst, (iii) disseminated this research to the National Institute for Advanced Transportation Technology (NIATT) via presentations and reports.

Future work (funding dependent) will focus on (i) optimizing the NS catalyst for higher C conversion efficiencies, (ii) upscale the reactor to fully evaluate the products as a drop-in fuel, and (iii) feasibility study for commercialization of the technology.

DESCRIPTION OF PROBLEM

Annually, approximately 27 billion tons of CO_2 is emitted from the burning of fossil fuels, and this is projected to increase by 60% by 2030. Therefore, using bioderived fuels is crucial to reducing the carbon footprint. The conversion of biomass into transportation fuels is a national priority with the Energy Independence and Security Act of 2007 (EISA), which requires the production of at least 36 billion gallons of renewable fuels by 2022. The novelty of the proposed project is to utilize biomass thermal conversion technologies for the production of high-energy liquid fuels, which will have a large impact on the environment and the nation's economy.

We will investigate alternative ways to utilize this biomass material to produce biofuels. Thermal gasification of biomass can typically convert >80% of biomass into synthesis gas (syngas) and the remainder as biochar (<20%). Mobile thermal conversion units can utilize this biomass through conversion to syngas, reducing transport volumes by more than 70%. This would increase supply chain efficiencies and decrease transport costs by an estimated 30% compared to transporting raw biomass to processing facilities, thus increasing economic viability of biofuel production from dispersed biomass feedstocks and reducing the dependency on petroleum.

To address the problem, we aim to develop Fischer-Tropsch (FT) type catalytic surfaces on nanospring (NS) supported structures that would improve the performance of the catalytic conversion of biomass-derived synthesis gas (syngas) into biofuels. This proposed central hypothesis will be tested through the following research objectives:

- Develop NS-based FT catalysts.
- Evaluate the NS-FT catalysts for the conversion of syngas into liquid fuels.
- Evaluate the synthesized liquid fuels.

APPROACH AND METHODOLOGY

Catalyst Preparation

Commercial silica gel (40-63 μm, Geduran) was used as support material for the conventional FTS catalyst. The 15 wt% Co/SiO_2-gel catalyst was prepared using incipient wetness impregnation method (also known as capillary impregnation because the amount of solution used here is just sufficient to fill the support pore volume) with solution of cobalt nitrate ($Co(NO_3)_2 \cdot 6H_2O$) (Adesina, 1996). After impregnation, the catalyst was dried under a vacuum in a rotary evaporator, first at 60°C and then as the temperature was slowly increased to 100°C. Subsequently, the catalyst was calcined in air at 400°C for 4 h.

Nanospring (NS)-supported Co catalysts were prepared in Dr. David McIlroy's lab in the physics department. At first, NSs were grown on a quartz frit (10 nm dia, grade 0) using the process developed by McIlroy et al. (2004). The deposition of Co on the support was performed by a thermal assisted reduction process. 150 μL of the $Co(NO_3)_2 \cdot 6H_2O$/ethanol solution (5 mg/mL) were dropped onto the support and dried in air at room temperature. Subsequently, catalysts were baked in a preheated tube furnace in a flow of Ar/H_2 mixture (140 mL/h, $Ar/H_2 = 13$) at 500°C and atmospheric pressure for 15 min, and then cooled down to room temperature. After repeating the above step three times, ~15% Co/SiO_2-NS catalysts were obtained.

Catalyst Characterization

Scanning Electron Microscopy-Energy Dispersive Spectroscopy (SEM/EDS)

Field emission SEM studies were performed using a Leo Supra 35 SEM (Thermo Fischer, USA) equipped with an EDS detector. The powder- and frit-type samples were mounted on the standard specimen stubs with the help of carbon double-sided adhesive tape.

Transmission Electron Microscopy (TEM)

Morphologies of supports and catalysts were characterized by TEM (Jeol Model JEM-2010 Electron Microscope, 200kV). Sample specimens for TEM tests were prepared by dispersion

of the catalysts in ethanol and the suspension dropped onto a copper grid. Several micrographs were recorded for each sample and analyzed to determine the Co particle size.

N_2 Physisorption

The specific surface area, pore volume, and average pore radius of the supports and catalysts were determined by N_2 physisorption (Micromeritics TriStar II 3020) in the laboratory of Professor Y. Wang at Washington State University. Prior to the analysis, samples were degassed at 300°C for 1 h under a vacuum. The specific surface area was obtained using the Brunauer-Emmett-Teller (BET) model.

X-ray Powder Diffraction (XRD)

The XRD patterns were obtained using a Siemens D5000 powder diffractometer with Cu/Kα radiation (λ = 1.54 Å). The spectra were recorded from 2θ = 25° to 80° with 0.01° step using a 1.00 s acquisition time per step. The average crystallite size of Co_3O_4 was calculated according to Scherrer's equation:

$$d = \frac{K\lambda}{\beta cos\theta} \quad (1)$$

where, K is the shape factor (K=1), λ is the wavelength of X-ray, β is the line broadening at half the maximum intensity (FWHM) in radians, and θ is the Bragg angle.

H_2-Temperature Programmed Reduction (H_2-TPR)

H_2-TPR spectra of the catalysts were recorded using a Micromeritics AutoChem II 2920 Chemisorption Analyzer, equipped with a thermal conductivity detector (TCD) in the laboratory of Professor Y. Wang at Washington State University. A sample (50 mg) was loaded in a U-shape quartz reactor and first purged in a flow of He (50 mL/min) at 250°C for 1 h to remove the trace amount of water, and then cooled down to 50°C. After purging, a 10% H_2/Ar mixture (50 mL/min) was introduced and the sample was heated to 800°C with a ramp of 10°C/min.

Catalyst Evaluation

The FTS performance of both Co/SiO_2-gel (0.2g) and Co/SiO_2-NS (0.2g including frits) catalysts was evaluated in a quartz fix-bed micro-reactor (Figure 1). Prior to the reaction, both catalysts were pretreated at atmospheric pressure by reduction with pure H_2 at 400°C for 12 h. After reduction, the reactor was operated at 230°C and atmospheric pressure. Syngas with a flow rate of 60 mL/min (H_2/CO ratio of 2) and N_2 used as internal standard (IS) with a flow rate of 10 mL/min were introduced from the top of the fix-bed reactor. Products were collected with a three-stage cold trap under liquid nitrogen every 10 h. The uncondensed vapor stream was collected at the end of the trap with a gas-sampling bag.

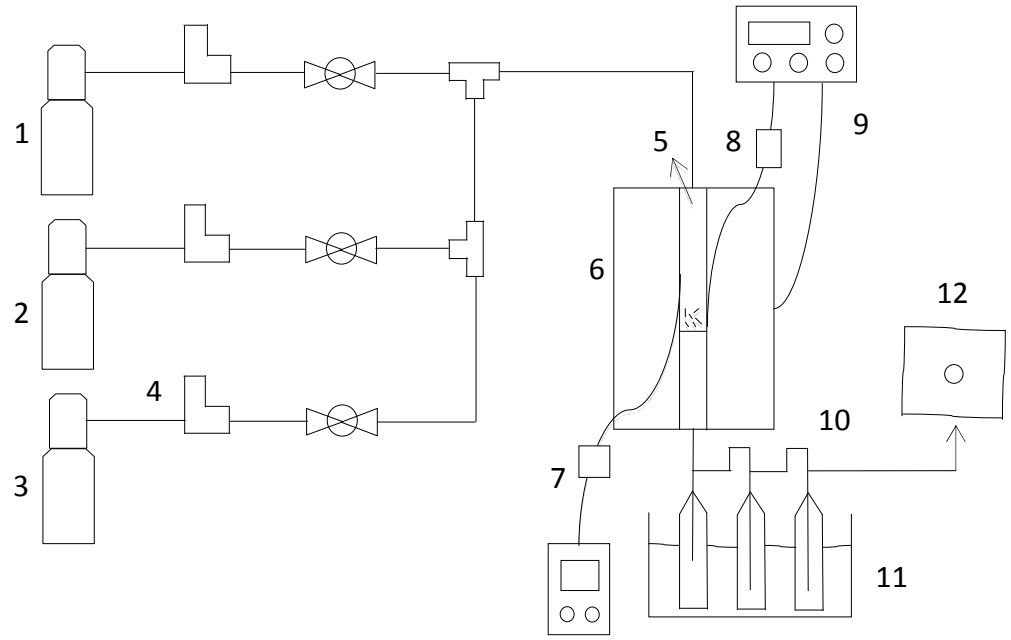

Figure 1: Schematic diagram of FTS reactor.

(1) CO cylinder; (2) H_2 cylinder; (3) N_2 cylinder; (4) mass flow controller; (5) quartz tubular reactor; (6) furnace; (7) K-type thermocouple; (8) J-type thermocouple; (9) temperature controller; (10) 3-stage condenser; (11) liquid N_2 bath; (12) gas sampling bag.

Condensed liquid products were analyzed by GC/MS (Focus-ISQ, ThermoScientific). Separation was achieved on a RTx-5ms (2.5 mm ID x 30 m, Restek) with He carrier gas and a temperature program of 40°C ramped to 200°C at 5°C/min. The Xcalibur v2 software was

used to analyze the data. Compounds were identified by their mass spectra, library mass spectral matching (NIST 2008) and retention time of known standard n-alkanes. 1, 2, 4-trichlorobenzene was used for quantification. GC/TCD (GOWMAC, Series 350) packed with HaySep DB column (30' x 1/8" x 0.085") was used for the analysis of gaseous products. The temperature of the detector was 175°C. Standard curve was prepared from individual gas (i.e. N_2, CO, CO_2, n-alkanes (C_1-C_2)) for quantification.

Catalytic activity, product selectivity and stability of the catalysts were monitored during the reaction period of 120 h. Activity was reported as CO conversion rate (Equation 2). C_{5+} selectivity was calculated by subtracting the amount of C_1-C_4 hydrocarbons and CO_2 in the product gas mixture from the total mass balance (Equation 3).

$$CO\ Conversion\ (\%) = \frac{CO_{In}\ -\ CO_{Out}}{CO_{In}} \times\ 100\% \qquad (2)$$

$$C_{5+}\ Selectivity\ (\%) =\ 100 - CO_2\ selectivity\ (\%) - (C_1 - C_4)\ selectivity\ (\%) \qquad (3)$$

FINDINGS

Catalyst Characterizations

SEM/EDS and TEM

Morphologies of both Co/SiO_2-gel and Co/SiO_2-NS catalysts were characterized by SEM and TEM, which were shown in Figure 2 and Figure 3, respectively. It can be found that the structure of SiO_2-gel support was significantly different from that of SiO_2-NS support. SiO_2-NS support materials were composed of randomly oriented nanowires, and the individual nanowire had a helical structure. Because of the unique helical structure, SiO_2-NS support had a major advantage over the conventional SiO_2-gel support, that is, it had 100% accessible surface area with zero closed porosity (Cantrell et al., 2011). In TEM images, agglomerations of Co particles were observed for Co/SiO_2-gel catalyst (Figure 3 (a)) whilst Co particles were uniformly coated on the surface of an individual NS (Figure 3 (b)). In addition, several TEM micrographs were recorded for each catalyst and measured to determine the particle size, which were listed in Table 1. Co_3O_4 particle size on Co/SiO_2-gel catalyst (14.7 nm) was larger than that on Co/SiO_2-NS catalyst (4.5 nm).

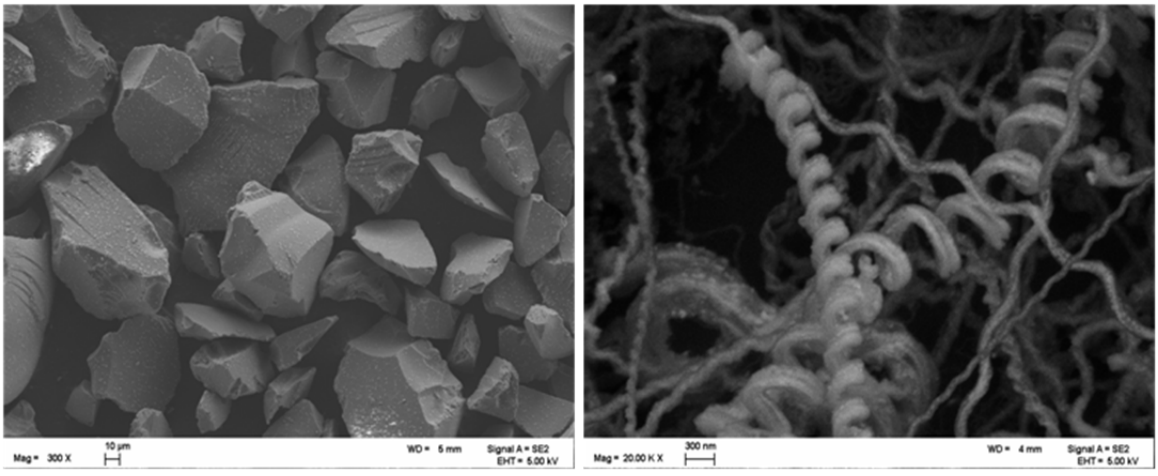

Figure 2: SEM micrograph of (a) Co/SiO_2-gel (300 ×) and (b) Co/SiO_2-NS (20K ×) catalysts.

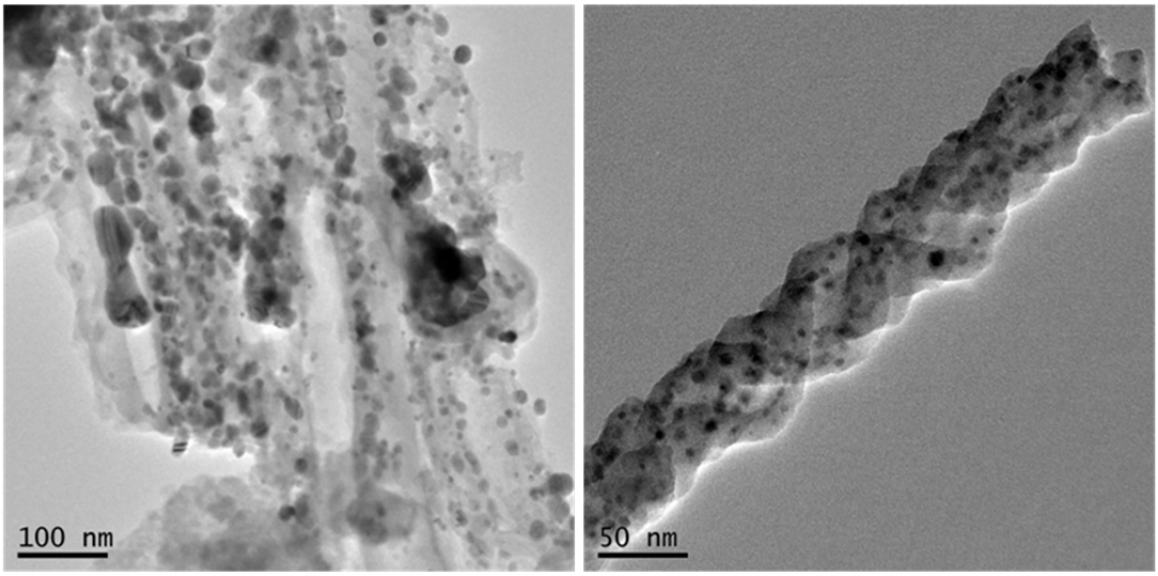

Figure 3: TEM image of (a) Co/SiO_2-gel (25K ×) and (b) Co/SiO_2-NS (50K ×) catalysts.

N_2 Physisorption

The BET specific surface area, porosity of supports, and supported Co catalysts were characterized by N_2 physisorption, which were listed in Table 1. SiO_2-gel had larger BET surface area and pore volume (478 m^2/g, 0.82 cm^3/g) than SiO_2-NS support materials. After loading with Co, the BET surface area and pore volume of both catalysts decreased significantly, indicating the blockage of the pores by the deposited Co particles.

Table 1: BET Surface Area, Porosity, Co_3O_4 Crystallite Size of Supports or/and Catalysts

supports/catalysts	BET (m^2/g)	pore volume (cm^3/g)	Co_3O_4 crystallite size (nm) -- TEM	Co_3O_4 crystallite size (nm) -- XRD
SiO_2-gel	478	0.82	--	--
SiO_2-NS	329	0.42	--	--
Co/ SiO_2-gel	370	0.62	14.7	13.1
Co/ SiO_2-NS	208	0.29	8.0	22.0

XRD

XRD patterns both Co/SiO_2-gel and Co/SiO_2-NS catalysts were presented in Figure 4. In the spectrum of Co/SiO_2-gel catalyst, the peaks at 2θ = 19.1°, 31.3°, 36.8°, 44.9°, 59.6° and 65.2° were related to different crystal planes of Co_3O_4 (Pan et al., 2010; Tang et al., 2012).

For Co/SiO2-NS catalyst, Co_3O_4 diffraction peaks showed at 2θ = 18.7°, 38.2°, 44.4°, and 64.7°. Relatively weak Co_3O_4 diffraction peaks showed in Co/SiO_2-NS catalyst, indicating that the Co species were better dispersed. Diffraction peak (440) was chosen to calculate Co_3O_4 particle size according to Scherrer's equation (Khodakov et al., 2003). The Co_3O_4 particle size were 13.1 nm and 12.7 nm for Co/SiO_2-gel and Co/SiO_2-NS catalysts (Table 1), respectively, which were in agreement with the results derived from TEM.

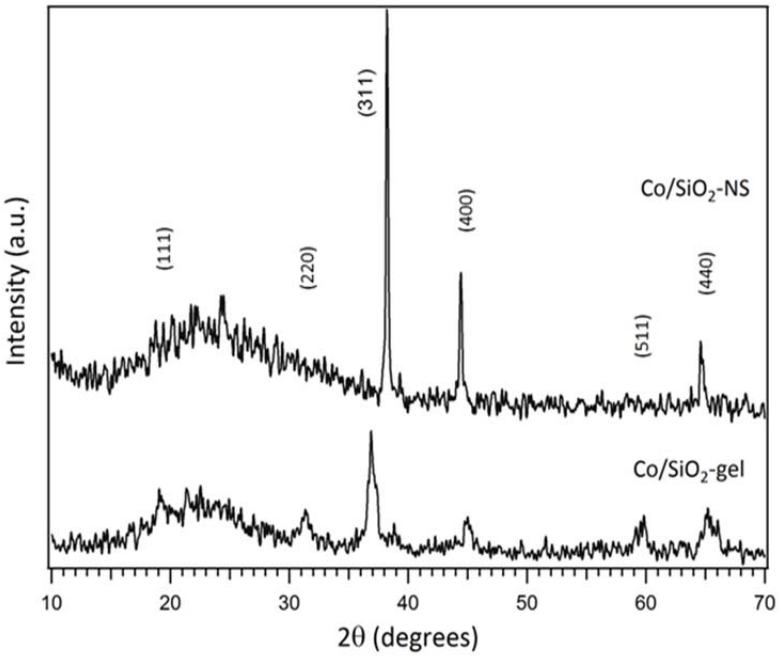

Figure 4: XRD diffractograms of both Co/SiO_2-gel and Co/SiO_2-NS catalysts.

H_2-TPR

TPR is an effective method to study the metal reduction behavior on the support. The H_2-TPR profiles of Co/SiO_2-gel and Co/SiO_2-NS catalysts are shown in Figure 5. In this figure, two peaks were observed in both catalysts. The first peak was attributed to the reduction of Co_3O_4 to CoO whilst the second peak was assigned to the reduction of CoO to Co^0 (Tavasoli et al., 2008). In the case of Co/SiO2-NS catalyst, two reduction peaks located at 391°C and 603°C, respectively. For Co/SiO_2-gel catalyst, lower reduction temperatures (278°C and 325°C) were observed, which was probably due to an easier reduction of larger cobalt

particles (TEM and XRD). Moreover, for Co/SiO_2-NS catalyst, both peaks had low intensity, which can be due to the small amounts of samples used for testing.

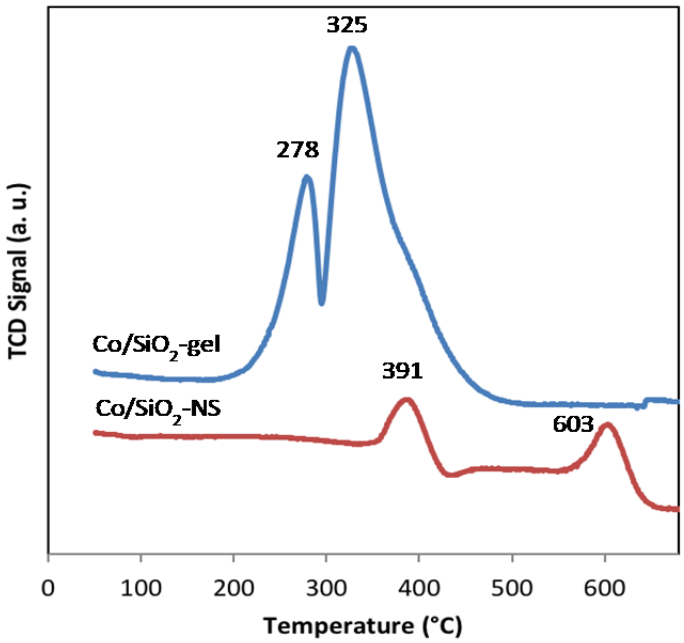

Figure 5: TPR profiles of both Co/SiO_2-gel and Co/SiO_2-NS catalysts.

Catalyst Activity and Selectivity

The first part of this project was to design and fabricate the quartz fix-bed micro-reactor and reaction product trapping system (Figure 1) to evaluate the catalyst performance and was successfully achieved. The syngas reaction products for both conventional and NS based FT catalysts were collected and analyzed for semi-volatiles by GC-MS analysis (C_6-C_{18}) and gases by GC-TCD (C_1-C_2). The GC-MS results show that both catalyst types produced alkanes with a similar product profile (Figure 6, Table 2). The products ranged from C_1 to C_{18}. The semi-volatile products will be a suitable substrate for diesel (typical range between C_6-C_{24}). CO conversion rate and product selectivity of both catalysts during the 50 -120 h period is given in Table 3. The CO conversion rate was up to about 84.62% and 66.41% for Co/SiO_2-gel and Co/SiO_2-NS catalysts, respectively. FTS activity rate is also based on the amounts of catalysts used in the process. About 40 times more Co/SiO_2-gel catalysts were used for evaluation than Co/SiO_2-NS catalysts; therefore, Co/SiO_2-NS catalyst showed

relatively higher FTS activity. Moreover, due to H_2-TPR profile, at the activation temperature of 400 °C, Co/SiO_2-NS catalyst cannot be fully reduced. Then, it can be concluded the higher FTS activity achieved from Co/SiO_2-NS catalyst mainly resulted from the 100% accessible surface area of novel NS support material that contributed more active sites. In addition, as given in Table 3, CH_4 and CO_2 selectivity for Co/SiO_2-NS catalyst were higher than that for Co/SiO_2-gel catalyst. Higher CO_2 selectivity indicated relatively higher water-gas-shift activity for Co/SiO_2-NS catalyst.

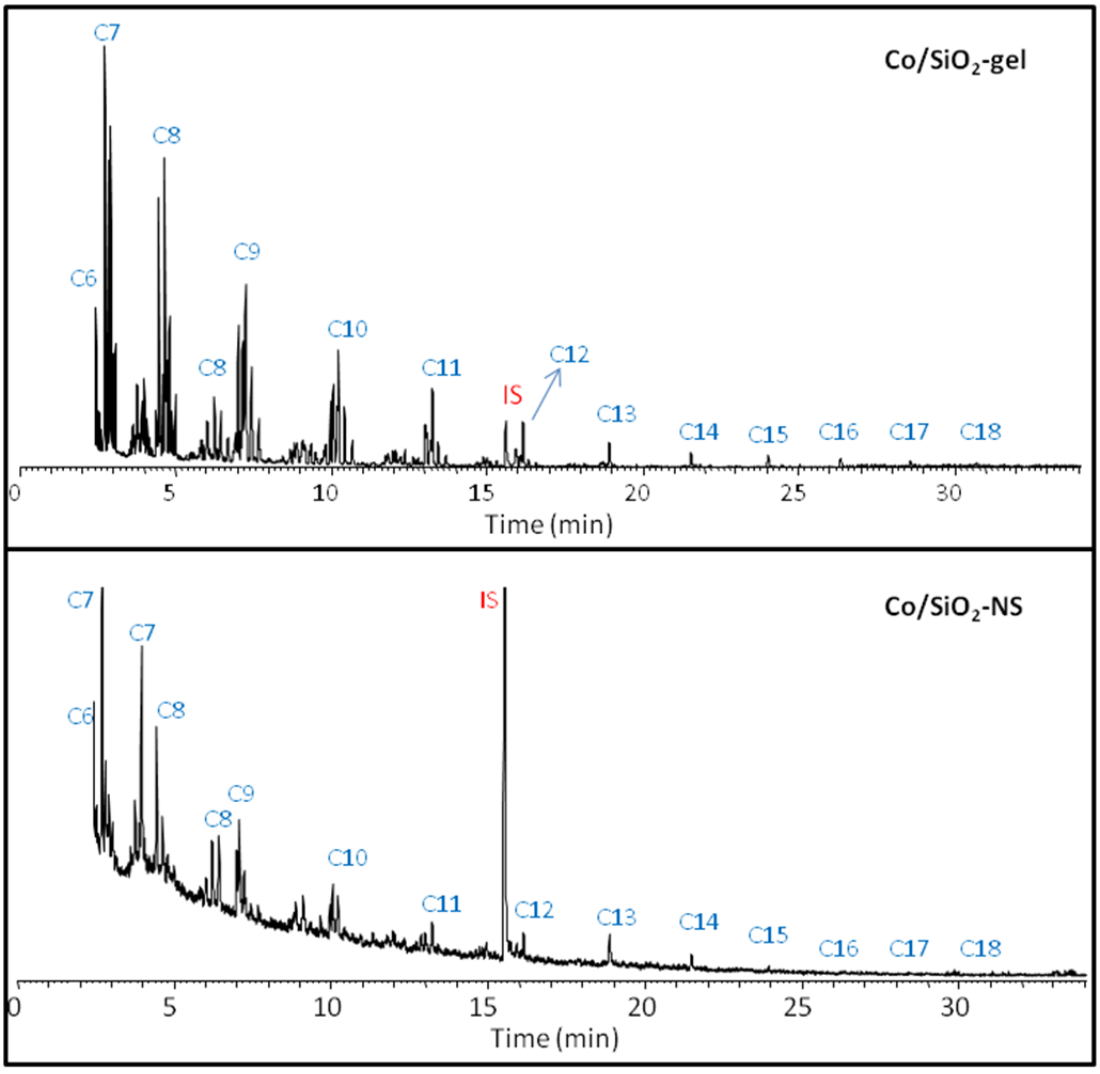

Figure 6: GCMS chromatograms of hydrocarbon reaction products from conventional (top) and nanospring (bottom) based FT catalysts.

Due to the limited separation capability of GC column, C_2-C_4 hydrocarbons were not identified and quantified, which probably contributed to 5-10% of total product yield. Generally, C_5+ hydrocarbon yield rate is calculated based on equations 2 and 3; therefore, it was not obtained here. However, the yield rate of n-alkanes (C_6-C_{18}) and aromatics (C_6-C_{10}) were calculated (Table 2). It can be observed that selectivity of them was very low, indicating n-alkanes and aromatics were not major components of syngas reaction products from both catalysts. Taking the amounts of catalysts into consideration, selectivity of those n-alkanes and aromatics for both catalysts were similar. Distribution of those n-alkanes for Co/SiO_2-gel and Co/SiO_2-NS catalysts is shown in Figure 7. Both catalysts showed similar distribution of n-alkanes favoring lighter components.

Table 2: GC Retention Time and Molecular Ion of N-Alkanes (C_6-C_{18})

Compounds	Formula	Retention time (min)	Molecular ion (M^+, m/z)
n-Hexane	C_6H_{14}	2.44	86
n-Heptane	C_7H_{16}	2.79	100
n-Octane	C_8H_{18}	4.57	114
n-Nonane	C_9H_{20}	7.16	128
n-Decane	$C_{10}H_{22}$	10.13	142
n-Undecane	$C_{11}H_{24}$	13.14	156
1,2,4-Trichlorobenzene (I.S.)	$C_6H_3Cl_3$	15.47	181
n-Dodecane	$C_{12}H_{26}$	16.05	170
n-Tetradecane	$C_{14}H_{30}$	21.42	198
n-Hexadecane	$C_{16}H_{34}$	26.23	226
n-Octadecane	$C_{18}H_{38}$	30.55	254

Table 3: CO Conversion and Product Selectivity of Co/SiO_2-gel and Co/SiO_2-NS Catalysts

Time period (h)	CO Conv. Rate (%) [a]		CH4 (%) [a]		CO2 (%) [a]		C_6-C_{18} n-alkanes, C_6-C_{10} aromatics (%) [b]	
	Gel-	NS-	Gel-	NS-	Gel-	NS-	Gel-	NS-
50-60	45.60	58.54	0.11	0.07	0.00	0.08	0.0068	0.0002
60-70	50.16	66.41	0.15	0.10	0.10	0.15	0.0056	0.0002
70-80	84.62	31.24	0.17	0.05	0.10	0.09	0.0049	0.0003
80-90	50.83	24.69	0.12	0.04	0.10	0.04	0.0048	0.0003
90-100	35.73	26.83	0.11	0.05	0.10	0.03	0.0033	0.0004
100-110	43.91	24.47	0.11	0.04	0.00	0.04	0.0052	0.0003
110-120	24.31	20.64	0.08	0.02	0.00	0.04	0.0042	0.0004

*a: gas products were collected from the last 1h of each time period, and the selectivity is volume percentage;
b: selectivity is weight percentage.

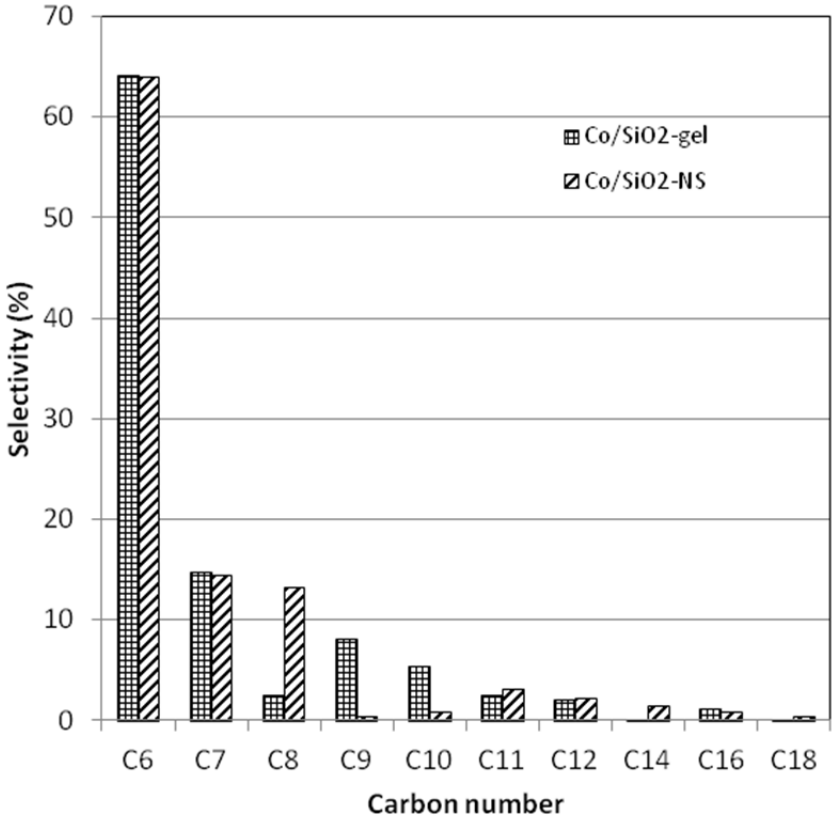

Figure 7: Distribution of n-alkanes (C_6-C_{18}) for Co/SiO_2-gel and Co/SiO_2-NS catalysts.

CONCLUSIONS

We were successful in developing a micro-reactor system to evaluate catalysts for FTS conversion of syngas into liquid fuels. We prepared and evaluated conventional silica gel supported Co FT catalyst and: (i) developed chemical tools to characterize catalysts, (ii) established FTS processing parameters for the micro-reactor system, (iii) developed protocols for trapping FTS reaction products and their characterization, and (iv) used this catalyst as a benchmark for the nanocatalysts. The FTS products were hydrocarbons ranging from C_1 to C_{18} which are in the range of diesel (C_6-C_{24}).

We were successful in synthesizing NS on a porous quartz frit bed and then coating the NS with Co nanoparticles at loadings between 13 and 50%. The NS-Co catalyst was successful in converting syngas into hydrocarbons (C_1–C_{18}). This proof of principle study has proven that NS-catalysts can produce "drop-in" biofuels.

RECOMMENDATIONS

The NS-Co FTS catalysts were shown to be successful in making drop-in biofuels. The next steps are to:

- Optimize the NS-Co catalyst for improving the C conversion efficiencies for making hydrocarbons.
- Establish the life-span of the NS-Co FTS catalyst.
- Upscale the amount of NS-Co catalyst synthesized for evaluating the FTS in a larger scale reactor to establish processing parameters.
- Undertake detailed chemical/fuel analysis of the FTS hydrocarbons for its suitability as a drop-in fuel.
- Undertake feasibility study on the engineering and economic requirements for the commercialization of the NS-Co FTS catalyst on small biomass gasifiers.

APPENDIX

References

Adesina A. A. 1996. Hydrocarbon synthesis via Fischer-Tropsch reaction: travails and triumphs. *Applied Catalysis A: General*, 138: 345-367.

Cantrell T. C., Corti G., Hyatt D. C., McIlroy D. N., Norton M. G., Prakash T., and Yahvah M. 2011. Nanosprings^{TM}: A versatile nanomaterial platform. *The Strem Chemiker*, 25(2): 27-37.

de la Osa A. R. , de Lucas A., Romero A. Valverde J. L., and Sanchez P. 2011. Influence of the catalytic support on the industrial Fischer-Tropsch synthetic diesel production. *Catalysis Today*, 176: 298-302.

de la Osa A. R., de Lucas A., Sanchez-Silva L., Diaz-Maroto J., Valverde J. L., and Sanchez P. 2012. Performing the best composition of supported Co/SiC catalyst for selective FTS diesel production. *Fuel*, 95: 587-598.

Dry M. E. 2002. The Fischer-Tropsch process: 1950-2000. *Catalysis Today*, 71: 227-241.

Enache D. I., Roy-Auberger M., and Revel R. 2004. Differences in the characteristics and catalytic properties of cobalt-based Fischer-Tropsch catalysts supported on zirconia and alumina. *Applied Catalysis A: General*, 268: 51-60.

Energy Information Administration (EIA). 2010. Annual Energy Review. U.S. Department of Energy.

Gonzalez-Carballo J.M. and Fierro J. L. G. 2010. Chapter 1: Fundamentals of Syngas Production and Fischer-Tropsch Synthesis. In: Biofuels from Fischer-Tropsch Synthesis – Ojeda M. and Rojas S. ed. Nova Science Publishers, Inc.

Jacobs G., Das T. K., Zhang Y., Li J., Racoillet G., Davis B. H. 2003. Fischer-Tropsch synthesis: support, loading, and promoter effects on the reducibility of cobalt catalysts. *Applied Catalysis A: General*, 233: 263-281.

Jones V. K., Neubauer L. R., and Bartholomew C. H. 1986. Effects of crystallite size and support on the CO hydrogenation activity/selectivity properties of Fe/carbon. *Journal of Physical Chemistry*, 90(4): 4832-4839.

Khodakov A. Y., Griboval-Constant A., Rechara R., and Zholobeno V. L. 2002. Pore size effects in Fischer-Tropsch synthesis over cobalt-supported mesoporous silicas. *Journal of Catalysis*, 206: 230-241.

Khodakov A. Y., Bechara R., and Griboval-Constant A. 2003. Fischer-Tropsch synthesis over silica support cobalt catalsyts: mesoporous structure versus cobalt surface density. *Applied Catalysis A: General*, 254(2): 273-288.

McIlroy D. N., Alkhateeb A., Zhang d., Aston D. E., Marcy A. C., and Norton M.G. 2004. Nanospring formation-unexpected catalyst mediated growth. *Journal of Physics: Condensed Matter*, 16(12): R415-R440.

Pan L., Xu M., and Zhang Z. D. 2010. Synthesis and electrocatalytic properties of Co3O4 nanocrystallites with various morphologies. *Journal of Cluster Science*, 21(4): 655-667.

Perego C. 2007. Development of a Fischer-Tropsch catalyst: from laboratory to commercial scale demonstration. *Rendiconti Lincei*, 18(4): 305-317.

Reuel R. C. and Bartholomew C. H. 1984. Effects of support and dispersion on the CO hydrogenation activity/selectivity properties of cobalt. *Journal of Catalysis*, 85(1): 78-88.

Schilke K. F., Wilson K. L., Cantrell T., Corti G., McIlroy D. N., and Kelly C. 2010. A novel enzyme microreactor with *Aspergillus oryzae* β-galactosidase immobilized on silicon dioxide nanosprings. *Biotechnology Progress*, 26(6): 1597-1605.

Serp P., Corrias M., and Kalck P. 2003. Carbon nanotubes and nanofibers in catalysis. *Applied Catalysis A: General*, 253: 337-358.

Tang H. Q., Liew K. Y., and Li J. L. 2012. Cobalt catalysts supported on silica nanotubes for Fischer-Tropsch synthesis. *Science China-Chemistry*, 55(1): 145-150.

Tavasoli A., Malek Abbaslou R. M., Trepanier M., and Dalai A. K. 2008. Fischer-Tropsch synthesis over cobalt supported on carbon nanotubes in a slurry reactor. *Applied Catalysis A: General*, 345: 134-142.

Tavasoli A., Sadagiani K., Khorashe F., Seifkordi A. A., Rohani A. A., and Nakhaeipour A. 2008. Cobalt supported on nanotubes – A promising novel Fischer-Tropsch catalyst. *Fuel Processing Technology*, 89: 491-498.

Vannice M. A. 1975. The catalytic synthesis of hydrocarbons from H2/CO mixtures over the Group VIII metals: I. The specific activities and product distributions of supported metals. *Journal of Catalysis*, 37(3): 449-461.

Wang Y., Noguchi M., Takahashi Y., and Ohtsuka Y. 2001. Synthesis of SBA-15 with different pore sizes and the utilization as supports of high loading of cobalt catalysts. *Catalysis Today*, 68: 3-9.

Zhang X., Liu Y., Liu G., Tao K., Jin Q., Meng F., Wang D., and Tsubaki N. 2012. Product distributions including hydrocarbon and oxygenates of Fischer-Tropsch synthesis over mesoporous MnO_2-supported Fe catalyst. *Fuel*, 92 (1): 122-129.